A New Gd^{3+} Spin Label for Gd^{3+}-Gd^{3+} Distance Measurements in Proteins Produces Narrow Distance Distributions

Elwy H. Abdelkader[a,†], Michael D. Lee[b,†], Akiva Feintuch[c], Marie Ramirez Cohen[c], James D. Swarbrick[b], Gottfried Otting[a,*], Bim Graham[b,*], Daniella Goldfarb[c,*]

[a]*Research School of Chemistry, Australian National University, Canberra, ACT 2601 (Australia)*

[b]*Monash Institute of Pharmaceutical Sciences, Monash University, Parkville VIC 3052 (Australia)*

[c]*Department of Chemical Physics, Weizmann Institute of Science, Rehovot 76100 (Israel)*

AUTHOR INFORMATION

Corresponding Authors

Gottfried Otting, e-mail: gottfried.otting@anu.edu.au

Bim Graham, e-mail: bim.graham@monash.edu.au

Daniella Goldfarb, e-mail : daniella.goldfarb@weizmann.ac.il

ABSTRACT

Gd^{3+} tags have been shown to be useful for performing distance measurements in biomolecules via the double electron-electron resonance (DEER) technique at Q- and W-band frequencies. We introduce a new cyclen-based Gd^{3+} tag that exhibits a relatively narrow EPR spectrum, affording high sensitivity, and which yields exceptionally narrow Gd^{3+}-Gd^{3+} distance distributions in doubly tagged proteins owing to a very short tether. Both the maxima and widths of distance distributions measured for tagged mutants of the proteins ERp29 and T4 lysozyme, featuring Gd^{3+}-Gd^{3+} distances of *ca*. 6 and 4 nm respectively, were well reproduced by simulated distance distributions based on available crystal structures and sterically allowed rotamers of the tag. The precision of the position of the Gd^{3+} ion is comparable to that of the nitroxide radical in an MTSL-tagged protein and thus the new tag represents an attractive tool for performing accurate distance measurements and potentially probing protein conformational equilibria.

TOC GRAPHICS

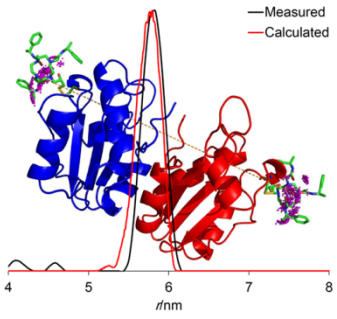

Double electron-electron resonance (DEER) has emerged as a powerful method in structural biology over the last decade because it provides distance distributions between spin labels inserted at well-defined sites within proteins and nucleic acids.[1,2] The spin labels are usually introduced through techniques of site-directed spin labeling (SDSL),[3] where the most popular method for attaching the spin label is via the thiol group of a native or genetically engineered cysteine residue. An alternative method is to employ an unnatural amino acid that has been genetically encoded to be incorporated in response to the amber stop codon.[4-6] So far, stable nitroxide radicals have been the most commonly used spin labels[7] for distance measurements using DEER.[8,9] The DEER measurement provides a distance distributions where its maximum give structural information while its width contains information on the conformational equilibria of the protein, provided that the label contribution to the width can be resolved. This becomes possible once the linker of the tag to the protein becomes short and preferably rigid. This motivated the design of rigid nitroxide labels[10] and recently a rigid labeling scheme employing Cu(II) was reported for proteins.[11] In recent years, Gd^{3+} (S = 7/2) spin labels have been introduced as an alternative to nitroxide spin labels for DEER measurements at Q- and W-band frequencies (about 32 and 95 GHz, respectively). The development of this new approach is driven by the high sensitivity these labels feature at high EPR frequencies and their reduction resistance in cellular environment. [12,13] Such measurements have been reported for model compounds,[15-18] proteins,[5,19-22] peptides in solution[23] and in membranes,[24,25] DNA[26] and nanoparticles.[27] Due to the greater bulkiness of the Gd^{3+} labels, compared to nitroxides, the labeling positions are usually restricted to exposed sites in the protein. Recently, Gd^{3+} ruler molecules with Gd^{3+}-Gd^{3+} distances in the range of 2.1–8.5 nm have been used to evaluate the validity of data analysis for this type of high-spin spin label.[17]. The development of Gd^{3+} spin labeling for DEER distance measurements has also opened up the

possibility to measure distances between different types of spin labels such as a Gd^{3+}-nitroxide pair, which delivers high sensitivity and allows measurement of several distances within the same sample. [27-30,31,32,33] Nonetheless, the approach of Gd^{3+} labeling is still under early stages of development and to realize its promise better Gd^{3+} tags with optimized spectroscopic and chemical properties should be designed. So far the majority of Gd^{3+}-Gd^{3+} distance measurements focused on rationalizing the maxima of the distance distribution[5,20,21] but not the width of the distribution, which so far has been rather broad. In this letter we introduce a new Gd^{3+} spin label that has the following combined unique features: (i) A small enough zero field splitting (ZFS) tensor that generates narrow central transition at 95 GHz that affords high sensitivity and (ii) A short linker to the protein that reduce considerably the width of the distance distribution and can be predicted.

The development of lanthanide tags for proteins was originally driven by applications in NMR spectroscopy, where tags with different paramagnetic lanthanides produce pseudocontact shifts that contain valuable long-range structural information.[34-39] When loaded with Gd^{3+} ions, such tags are usually also suitable for distance measurements by EPR, but the effectiveness of distance measurements in terms of sensitivity and structural information content critically depends on the chemical and spectroscopic properties of the Gd^{3+} tag. The ideal Gd^{3+} tag for DEER experiments should immobilize the metal ion close to the target molecule without affecting its structure. In addition, it should bind the metal ion very tightly and the metal should be fully coordinated to prevent hard-to-predict metal-mediated interactions with other parts of the protein or other molecules. Finally, it must be possible to incorporate the tag site-specifically and with a minimal number of additional modifications to the target molecule. Tags that ligate the Gd^{3+} ion with high thermodynamic and kinetic stability are particularly attractive as these tags can be loaded with Gd^{3+} prior to their ligation to the target protein, eliminating problems associated with Gd^{3+} titrations.[23]

Spectroscopically, the best Gd^{3+} tags should exhibit a small ZFS for maximal sensitivity. Such rigid tags, however, may require special considerations for short distances measurements owing to deviations from the weak coupling approximation used in the data analysis,[17] which introduces artificial broadening.

Tags based on 1,4,7,10-tetraazacyclododecane-1,4,7,10-tetraacetic acid ("DOTA") and its derivatives possess most of the desired properties and yield narrow EPR line widths and sufficiently long phase memory times. Several such tags have been explored for Gd^{3+}-Gd^{3+} distance measurements, namely MTS-ADO3A,[24] the maleimide DO3A tag[12] and the **C1** tag[20] shown in Fig. 1. In the **C1** tag, originally developed for paramagnetic NMR,[40] bulky phenylethylacetamide groups limit the tag's mobility through steric effects. All these tags, however, feature rather long, flexible tethers that allow rotation about four bonds between the Gd^{3+} ion and the S-S or C-S bond that links them to a cysteine residue in the protein. Long flexible tethers necessarily increase the widths of any distance distribution and thus limit the protein dependent information. In a first step towards an unnatural amino acid that positions the Gd^{3+} ion at a defined location, the **C3** tag[41] loaded with Gd^{3+} (Fig. 1) has recently been conjugated to *p*-azido-*L*-phenylalanine (AzF). Here, the metal position could be predicted very well from the three-dimensional structure of the protein by a single tag conformation.[5] The latter was established by the standard mutation tool in the program PyMOL to find the most likely AzF side-chain conformation[42] and assuming a fixed geometry of the ligation product. Compared with tags directed at cysteine, however, the ligation of the **C3** tag to an AzF residue results in a rather long, albeit rigid, tether between the protein and the Gd^{3+} ion, limiting the information content of Gd^{3+}-Gd^{3+} distance distributions measured in proteins of unknown structure.

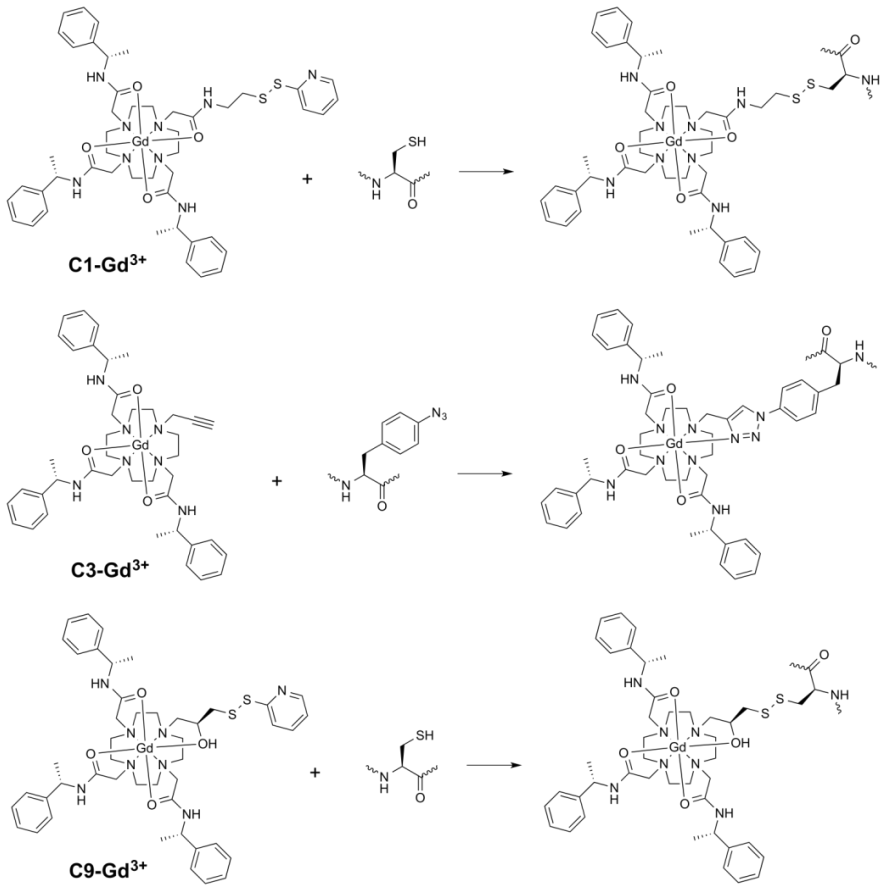

Fig. 1. Structures of the Gd^{3+} tags employed in this work. Each complex carries a 3+ charge.

Here we introduce a new DOTA-based Gd^{3+} tag, **C9** (Fig. 1), featuring a cysteine-conjugatable pendant arm with just two bonds prior to the disulfide bond, which minimizes the tag's contribution to the width of distance distribution. We demonstrate the performance of this tag on two mutants, S114C and G147C, of the protein ERp29, which forms a 51 kDa homodimer[20,43,44] and on the A93C/N140C mutant of T4 lysozyme. We further compare the results with those obtained from the **C1** and **C3** tags. We show that the **C9** tag features a narrow Gd^{3+}-Gd^{3+} distance distribution (0.4–0.6 nm, at half height), for both proteins that could be well reproduced by simple modelling, suggesting that this tag can be useful for providing both accurate structural information and

probing local flexibility in proteins, which is an important feature not yet reported for Gd^{3+} spin labels.

The **C9** tag is a hybrid design of **C1**[12] and another earlier reported tag, **C8**,[45] featuring the sterically bulky pendants of the former and the much shorter conjugatable linker of the latter. The synthesis of the tag is reported in the ESI. The "activated" pyridin-2-yldisulfanyl group within the **C9** tag reacts with a cysteine residue to form a disulfide bond between the tag and protein (Fig. 1). We obtained quantitative ligation yields. Details of the ligation conditions are reported in the ESI.

The W-band echo-detected (ED) EPR spectra of the S114C (or S114AzF) mutant of ERp29 with the different tags are depicted in Fig. 2. The width (at half height) of the central EPR transition exhibits the following trend: AzF-**C3** > **C9** > **C1,** indicating that **C3** has the largest ZFS parameter (*D*) value. This is expected considering that the Gd^{3+} coordination sphere in the **C3** tag lacks one of the oxygen donors, which is instead replaced with a nitrogen donor from the triazole ring. The phase memory time **C3** and **C9** are quite similar whereas that of C1 is slightly longer (See Fig. S6). The corresponding W-band DEER traces after background removal are shown in Fig. 3a and the derived distance distributions are given in Fig. 3b. The primary DEER data are presented in the ESI, Fig. S7.

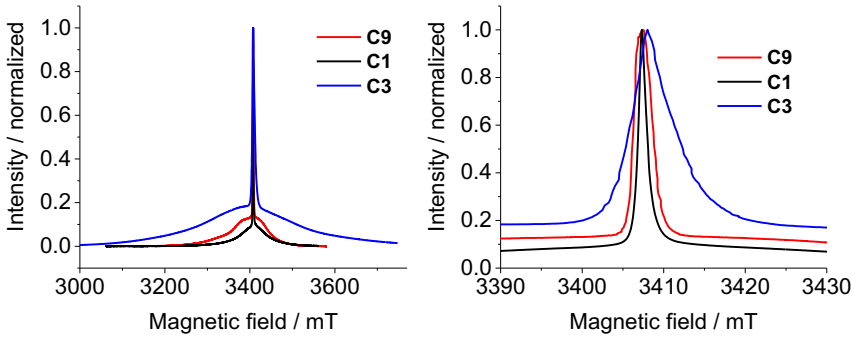

Fig. 2. W-band echo-detected EPR spectra of ERp29 S114C/S114AzF (pD = 4.9) with all the tags investigated recorded at 10 K. Left panel: full spectrum. Right panel: expanded plot of the central transition. The results for the **C1** tag are reproduced from ref. 20.

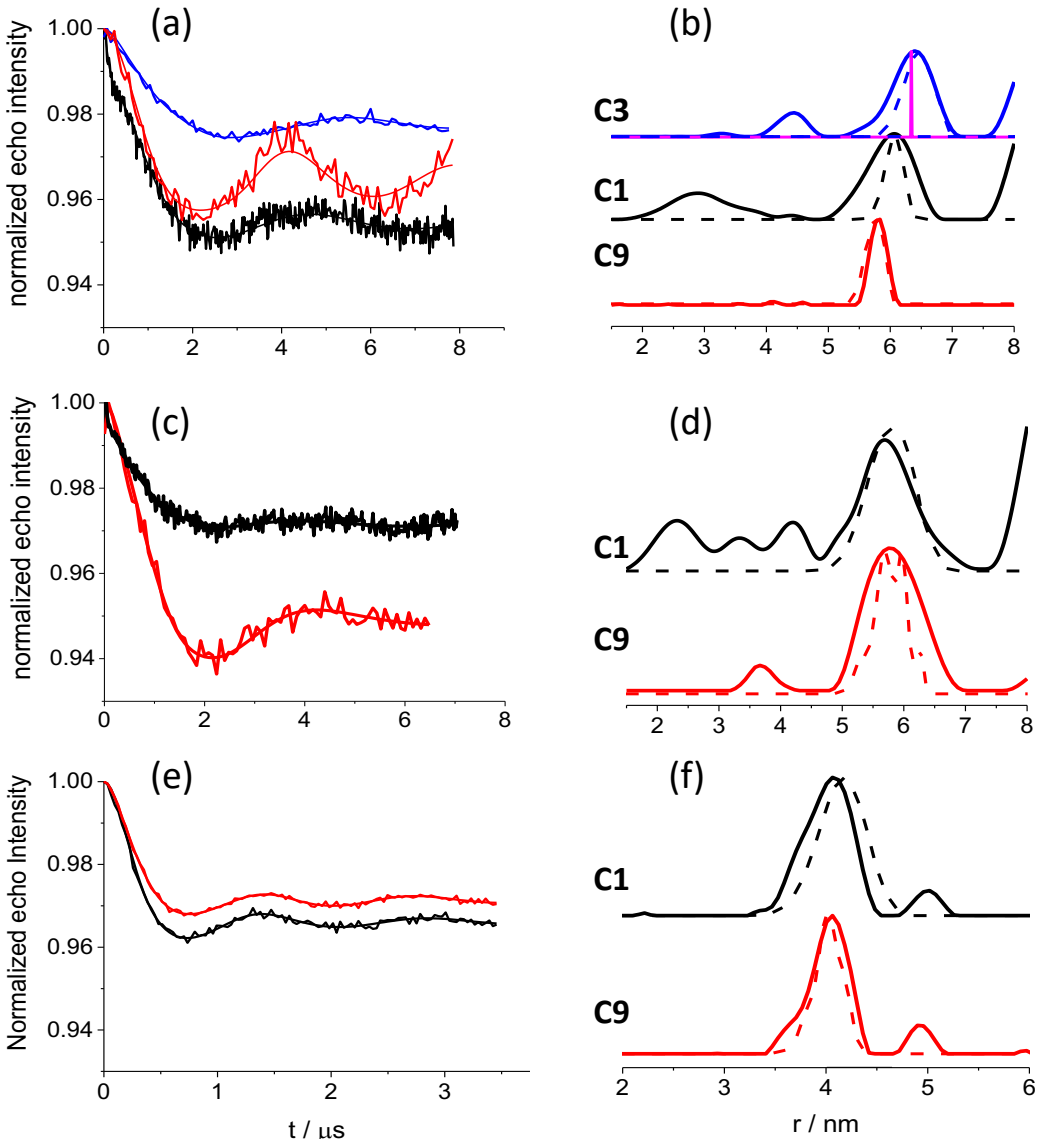

Fig. 3. W-band DEER data (10 K) of ERp29 S114C/S114AzF ligated with the different tags of Fig. 1 (pD = 4.9). (a) Data recorded with the four-pulse DEER sequence[9] and after background removal, including the fitted curve obtained with the distance distribution shown in (b). The vertical line (magenta) in (b) marks the distance predicted by modelling the tag with a single

conformation as described in ref. 5. (c) and (d) Corresponding results for the ERp29 G147C mutant, except that no data were recorded with the AzF-**C3** tag. The **C1** data were reproduced from ref. 20. (e) and (f) The same for T4 lysozyme A93C/N140C with **C9** and **C1** tags. The DEER data were analyzed with DeerAnalysis[46] and employing Tikhonov regularization. The dashed traces in (b), (d) and (f) represent the calculated distance distributions (see text for details).

The shallowest modulation depth was obtained with the AzF-**C3** tag, as expected from its broader ED-EPR spectrum. The distances indicated by the maxima of the distance distributions for this mutant follow the trend AzF-**C3** > **C1** > **C9**, in agreement with the different intrinsic lengths of the tethers between the Gd^{3+} ion and the protein backbone associated with these tags. In all cases, the maxima of the distance distributions were accurately predicted by modeling of the tag conformations using sterically allowed rotamers of the tag. In the case of the AzF-**C3** residue, the maximum of the distance distribution, shown as a single line in Fig. 3b, was readily predicted by a single tag conformation obtained by using the mutation tool of PyMOL to determine the dihedral angles χ_1 and χ_2, while keeping all other side chain dihedral angles in the conformation shown in Fig. S8.[5]

Among the three protein examples of Fig. 3, the **C9** tag produced the narrowest distribution widths of all tags for site 114 of ERp29 (Fig. 3b) and for a double-Cys mutant of T4 lysozyme (Fig. 3f). Moreover both distribution widths were accurately predicted by rotamer distributions (see below). In view of the rigidity of the tether of the AzF-**C3** residue, the width of the distance distribution observed with this tag was disappointing. To simulate the broad distance distribution shown in Fig. 3b we allowed free rotations about all side-chain dihedral angles (Fig. S7)). Similarly, the experimental distance distribution of the **C1** tag at the site of residue 114 of ERp29 was significantly greater than predicted (Fig. 3b). The difference must be associated with

properties of the C1 tag that are not taken into account by the simple modeling approach used.. The distance measurement with the **C1** tag in the T4 lysozyme mutant was also predicted with lesser accuracy than for the **C9** tag (Fig. 3f). Clearly, the small number of rotatable bonds in the **C9** tag contributes both to narrow distribution widths and more accurate prediction of the distance from the protein structure.

A comparison of the **C1** and **C9** tags was carried out for the ERp29 G147C mutant as well (Fig. 3c,d). There, the distance distributions are wider. Fundamentally, the width of a distance distribution is determined by two factors. One is protein-dependent and reflects the conformational backbone dynamics of the protein along with the local dynamics (mobility) of the residue carrying the label. The second is label-dependent and reflects all possible conformations of the label that are sterically compatible with the labeling site. Therefore, interpretation of the width of the distance distribution requires untangling the intrinsic contribution of protein dynamics from that of the label, and this is easier the more rigid the spin label is.[47,48] As a homodimer, ERp29 is particularly well suited for such an examination because the DEER distance distribution reflects the conformational equilibrium at only a single site. Accordingly, the width difference between the two sites reflects the greater solvent exposure of the 147 site that permits a wider range of spin label conformations and/or increased protein structural dynamics at this site.

The tag-specific contribution to the distance distribution can often adequately be simulated by a distance distribution that compiles all sterically allowed rotamers of the label,[15] or by considering a more elaborate rotamer library based on molecular dynamics simulations and crystal structures.[49] Accordingly, protein motion information has successfully been deduced from the width of distance distributions derived from DEER data on nitroxide spin labels,[50,51] but not yet using Gd^{3+} tags. To account for contributions to the distance distribution arising from greater solvent exposure, as

opposed to protein local motions, we modeled the distance distributions for all tags based on the crystal structures (PDB ID 2QC7 for ERp29[43] and 2LZM for T4 lysozyme[49]) and all possible conformations of the tag that avoided clashes with the protein (see ESI for details). The results show a remarkable agreement for **C9** at site 114 of ERp29 and the calculated distribution for site 147 is broader than for 114, reflecting the greater exposure of the site. Yet, for site 147 the experimental distance distribution for **C9** is wider than the modeled one, suggesting that there are contributions from local dynamics. However, we cannot exclude some broadening arising from uncertainties in the background removal due to insufficiently long evolution time. The difference in experimental distribution width is much less obvious for **C1**, which, like **C3**, produced an intrinsically greater width (we did not tag site 147 with **C3** because an AzF residue at this site is predicted to populate two different χ_1 angles).

To check whether the remarkably narrow width of the distance distributions obtained with the **C9** tag could be aided by electrostatic interactions with nearby carboxyl groups of the protein, we mutated Glu113 in the ERp29 S114C mutant to glutamine. In this mutant, the maximum of the distance distribution shifted slightly from 5.83 to 5.99 nm and the width increased by a small amount, from 0.4 to 0.5 nm (Fig. S9). These results indicate only a limited degree of interaction with Glu113. Upon changing the pD from 4.9 to 7, which may alter the protonation state and coordination properties of the OH groups in proximity of the Gd^{3+} ion (Fig. 1c),[45,52] the maximum of the distance distribution changed to 5.88 nm, and the width to 0.63 nm (Fig. S9), which is still considerably narrower than the widths observed for any of the other tags. The reproducibly narrow width of the distance distribution that can be achieved with the **C9** tag thus seems to be primarily associated with the short tether produced by this tag. For comparison, the distance distribution

width observed for a series of rigid rulers with Gd^{3+}-Gd^{3+} distances in the range of 3.4–8.3 was 0.4–0.7 nm.[17]

To explore whether the difference in the distance distribution widths observed with **C9** between sites 114 and 147 reflects solvent exposure and site-dependent protein mobility , we also labeled these two positions with a nitroxide spin label (MTSL). Here, we observed a much stronger orientation selection for site 114 than for site 147 (Fig. S10), which is consistent with the behavior of **C9**. In Figure 4 and S13 we compare the conformational space accessible to **C1, C9** and MTSL at site 114, showing that the **C9** tag samples a region of space that is smaller or comparable the MTSL nitroxide spin label. In addition to distance measurements, MTSL is sometimes used to probe protein mobility via DEER measurements.[44,51]

For a third example, we also labeled T4 lysozyme A93C/N140C with both **C1** and **C9** and compared their distance distributions (Fig. 3e,f,). Because of the shorter distances between the tags in this case (*ca*. 4 nm), the DEER measurements were carried out with very large $\Delta\nu$ ($\Delta\nu$ = 878 MHz for **C9** and 636 MHz for **C1**) in order to minimize potential artificial broadening induced by ignoring the contribution of the pseudosecular terms of the dipolar interaction[17] (it was anticipated that this contribution might be significant for a *ca*. 4 nm tag separation because of the narrow central transitions of **C9** and **C1** and the associated small ZFS). Like in the case of ERp29 S114C, **C9** showed close agreement between experimental and predicted distance distribution widths, as expected for a rigid intra-domain distance. In contrast to **C9**, to obtain a reasonable match between experimental and predicted distance distribution for **C1** a conformational bias of the tag due to electrostatic attraction with protein carboxyl groups was assumed (see Fig. 3f) (see Fig. S12 for the non-bias distance distribution).

To summarize, we have introduced a new Gd^{3+} tag, **C9**, that produces a short linkage to protein cysteine residues and a limited tag flexibility afforded by only two dihedral angles. Both the maximum and width of distance distributions obtained with this tag can be well accounted for and therefore it represents an attractive tool for obtaining accurate distance measurements and probing protein conformational equilibria.

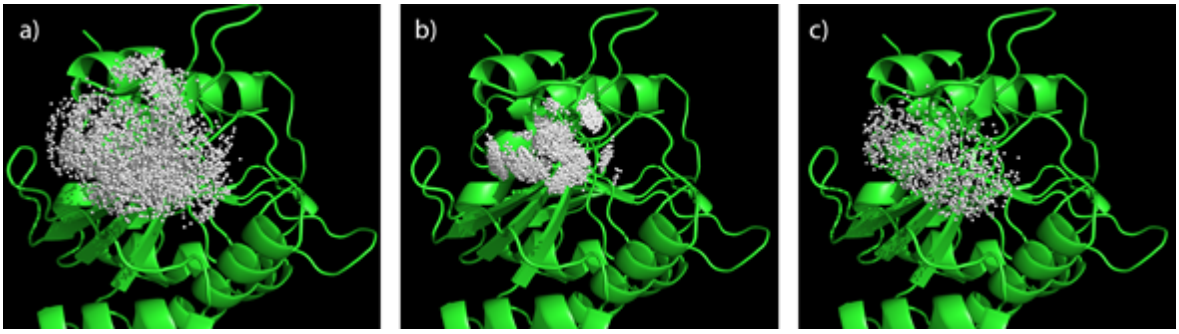

Fig. 4 Space accessible to the Gd^{3+} ion and nitroxide oxygen in the rotamer libraries generated for (a) the **C1**-**Gd**$^{3+}$ tag, (b) the **C9-Gd**$^{3+}$ tag, and (c) MTSL ligated to position 114 of ERp29. A single protein monomer is displayed in a ribbon representation. Balls identify the coordinates found for the Gd^{3+} ion and nitroxide oxygen in the rotamer libraries of the respective tags.

ACKNOWLEDGMENT

This work was supported by the Israel Science Foundation, the Australian Research Council (ARC), and an Australia-Weizmann Making Connections grant. B. G. thanks the ARC for a Future Fellowship (FT130100838). D. G. holds the Erich Klieger Professorial Chair in Physical Chemistry.

Supporting Information. Tag synthesis and characterization; sample preparation; experimental details for EPR and DEER measurements; raw DEER data for ERp29 and T4 ltsozyme; additional DEER data for ERp29; DEER data for ERp29 S114C labeled with MTSL; modeling details.

REFERENCES

(1) Borbat, P. P.; Freed , J. H. Pulse Dipolar Electron Spin Resonance: Distance Measurements. In *Struct. Bond.*; C. Timmel, Harmer, J., Eds.; Springer Berlin Heidelberg: 2013; Vol. 152, p 1-82.

(2) Jeschke, G.; Polyhach, Y. Distance Measurements on Spin-Labelled Biomacromolecules by Pulsed Electron Paramagnetic Resonance. *Phys. Chem. Chem. Phys.* **2007**, *9*, 1895-1910.

(3) Hubbell, W. L.; Gross, A.; Langen, R.; Lietzow, M. A. Recent Advances in Site-Directed Spin Labeling of Proteins. *Currr. Opin. Struct. Biol.* **1998**, *8*, 649-656.

(4) Chin, J. W.; Santoro, S. W.; Martin, A. B.; King, D. S.; Wang, L.; Schultz, P. G. Addition of P-Azido-L-Phenylalanine to the Genetic Code of Escherichia Coli. *J. Am. Chem. Soc.* **2002**, *124*, 9026-9027.

(5) Abdelkader, E. H.; Feintuch, A.; Yao, X.; Adams, L. A.; Aurelio, L.; Graham, B.; Goldfarb, D.; Otting, G. Protein Conformation by EPR Spectroscopy Using Lanthanide Tagging of Genetically Encoded Amino Acids. *Chem. Comm.* **2015,** *51,* 15898-15901

(6) Fleissner, M. R.; Brustad, E. M.; Kalai, T.; Altenbach, C.; Cascio, D.; Peters, F. B.; Hideg, K.; Peuker, S.; Schultz, P. G.; Hubbell, W. L. Site-Directed Spin Labeling of a Genetically Encoded Unnatural Amino Acid. *Proc. Natl. Acad. Sci. USA* **2009**, *106*, 21637-21642.

(7) Shelke, S. A.; Sigurdsson, S. T. Site-Directed Nitroxide Spin Labeling of Biopolymers. *Struct. Bond.* **2013**, *152*, 121-162.

(8) Milov, A. D.; Ponomarev, A. B.; Tsvetkov, Y. D. Electron Electron Double-Resonance in Electron-Spin Echo - Model Biradical Systems and the Sensitized Photolysis of Decalin. *Chem. Phys. Lett.* **1984**, *110*, 67-72.

(9) Pannier, M.; Veit, S.; Godt, A.; Jeschke, G.; Spiess, H. W. Dead-Time Free Measurement of Dipole-Dipole Interactions between Electron Spins. *J. Magn. Reson.* **2000**, *142*, 331-340.

(10) Fleissner, M. R.; Bridges, M. D.; Brooks, E. K.; Cascio, D.; Kalai, T.; Hideg, K.; Hubbell, W. L. Structure and Dynamics of a Conformationally Constrained Nitroxide Side Chain and Applications in EPR Spectroscopy. *Proc. Natl. Acad. Sci. U S A* **2011**, *108*, 16241-16246.

(11) Cunningham, T. F.; Putterman, M. R.; Desai, A.; Horne, W. S.; Saxena, S. The Double-Histidine Cu2+-Binding Motif: A Highly Rigid, Site-Specific Spin Probe for Electron Spin Resonance Distance Measurements. *Angew. Chem.-Intl Ed.* **2015**, *54*, 6330-6334.

(12) Martorana, A.; Bellapadrona, G.; Feintuch, A.; Di Gregorio, E.; Aime, S.; Goldfarb, D. Probing Protein Conformation in Cells by Epr Distance Measurements Using Gd3+ Spin Labeling *J. Am. Chem. Soc.* **2014**, *136* 13458-13465

(13) Qi, M.; Gross, A.; Jeschke, G.; Godt, A.; Drescher, M. Gd(Iii)-Pymta Label Is Suitable for in-Cell Epr. *J. Am. Chem. Soc.* **2014**, *136*, 15366-15378.

(14) Goldfarb, D. Gd3+ Spin Labeling for Distance Measurements by Pulse Epr Spectroscopy. *Phys. Chem. Chem. Phys.* **2014**, *16*, 9685-9699.

(15) Raitsimring, A. M.; Gunanathan, C.; Potapov, A.; Efremenko, I.; Martin, J. M. L.; Milstein, D.; Goldfarb, D. Gd3+ Complexes as Potential Spin Labels for High Field Pulsed Epr Distance Measurements. *J. Am. Chem. Soc.* **2007**, *129*, 14138-14140.

(16) Potapov, A.; Song, Y.; Meade, T. J.; Goldfarb, D.; Astashkin, A. V.; Raitsimring, A. Distance Measurements in Model Bis-Gd(Iii) Complexes with Flexible "Bridge". Emulation

of Biological Molecules Having Flexible Structure with Gd(Iii) Labels Attached. *J. Magn. Reson.* **2010**, *205*, 38-49.

(17) Dalaloyan, A.; Qi, M.; Ruthstein, R.; Vega, S.; Godt, A.; Feintuch, A.; Goldfarb, D. Gd(Iii)-Gd(Iii) Epr Distance Measurements – the Range of Accessible Distances and the Impact of the Zero Field Splitting. *Phys. Chem. Chem. Phys.* **2015**, *17*, 1464-18476.

(18) Doll, A.; Qi, M.; Pribitzer, S.; Wili, N.; Yulikov, M.; Godt, A.; Jeschke, G. Sensitivity Enhancement by Population Transfer in Gd(Iii) Spin Labels. *Phys. Chem. Chem. Phys.* **2015**, *17*, 7334-7344.

(19) Potapov, A.; Yagi, H.; Huber, T.; Jergic, S.; Dixon, N. E.; Otting, G.; Goldfarb, D. Nanometer-Scale Distance Measurements in Proteins Using Gd3+ Spin Labeling. *J. Am. Chem. Soc.* **2010**, *132*, 9040-9048.

(20) Yagi, H.; Banerjee, D.; Graham, B.; Huber, T.; Goldfarb, D.; Gottfried, O. Gadolinium Tagging for High-Precision Measurements of 6 Nm Dis-Tances in Protein Assemblies by EPR. *J. Am. Chem. Soc.* **2011**, *133*, 10418-10421

(21) Edwards, D. T.; Huber, T.; Hussain, S.; Stone, K. M.; Kinnebrew, M.; Kaminker, I.; Matalon, E.; Sherwin, M. S.; Goldfarb, D.; Han, S. Determining the Oligomeric Structure of Proteorhodopsin by Gd3+-Based Pulsed Dipolar Spectroscopy of Multiple Distances. *Structure* **2014**, *22*, 1677-1686.

(22) Barthelmes, D.; Granz, M.; Barthelmes, K.; Allen, K. N.; Imperiali, B.; Prisner, T.; Schwalbe, H. Encoded Loop-Lanthanide-Binding Tags for Long-Range Distance Measurements in Proteins by NMR and Epr Spectroscopy. *J. Biomol. NMR* **2015**.

(23) Gordon – Grossman, M.; Kaminker, I.; Gofman, Y.; Shai, Y.; Goldfarb, D. W-Band Pulse EPR Distance Measurements in Peptides Using Gd3+- Dipicolinic Acid Derivatives as Spin Labels. *Phys. Chem. Chem. Phys.* **2011**, *13*, 10771-10780.

(24) Matalon, E.; Huber, T.; Hagelueken, G.; Graham, B.; Feintuch, A.; Frydman, V.; Otting, G.; Goldfarb, D. Gd3+ Spin Labels for High Sensitivity Distance Measurements in Trans-Membrane Helices. *Angew. Chem. Int. Ed.* **2013**, *52,* 11831-11834

(25) Manukovsky, N.; Frydman, V.; Goldfarb, D. Gd3+-Spin Labels Report the Conformation and Solvent Accessibility of Solution and Vesicle-Bound Melittin. *J. Phys. Chem. B.* **2015**, *119*,13732-13741

(26) Song, Y.; Meade, T. J.; Astashkin, A. V.; Klein, E. L.; Enemark, J. H.; Raitsimring, A. Pulsed Dipolar Spectroscopy Distance Measurements in Biomacromolecules Labeled with Gd(Iii) Markers. *J. Magn. Reson.* **2011**, *210,* 59-68

(27) Yulikov, M.; Lueders, P.; Warsi, M. F.; Chechik, V.; Jeschke, G. Distance Measurements in Au Nanoparticles Functionalized with Nitroxide Radicals and Gd3+-Dtpa Chelate Complexes. *Phys. Chem. Chem. Phys.* **2012**, *14*, 10732-10746.

(28) Lueders, P.; Jager, H.; Hemminga, M. A.; Jeschke, G.; Yulikov, M. Distance Measurements on Orthogonally Spin-Labeled Membrane Spanning Walp23 Polypeptides. *J. Phys. Chem. B* **2013**, *117*, 2061-2068.

(29) Garbuio, L.; Bordignon, E.; Brooks, E. K.; Hubbell, W. L.; Jeschke, G.; Yulikov, M. Orthogonal Spin Labeling and Gd(Iii)-Nitroxide Distance Measurements on Bacteriophage T4-Lysozyme. *J. Phys. Chem. B* **2013**, *117*, 3145-3153.

(30) Lueders, P.; Jeschke, G.; Yulikov, M. Double Electron-Electron Resonance Measured between Gd(3+) Ions and Nitroxide Radicals. *J. Phys. Chem. Lett.* **2011**, *2*, 604-609.

(31) Kaminker, I.; Tkach, I.; Manukovsky, N.; Huber, T.; Yagi, H.; Otting, G.; Bennati, M.; Goldfarb, D. W-Band Orientation Selective Deer Measurements on a

Gd3+/Nitroxide Mixed-Labeled Protein Dimer with a Dual Mode Cavity. *J. Magn. Reson.* **2013**, *227*, 66-71.

(32) Kaminker, I.; Yagi, H.; Huber, T.; Feintuch, A.; Otting, G.; Goldfarb, D. Spectroscopic Selection of Distance Measurements in a Protein Dimer with Mixed Nitroxide and Gd3+ Spin Labels. *Phys. Chem. Chem. Phys.* **2012**, *14*, 4355-4358.

(33) Yulikov, M. Spectroscopically Orthogonal Spin Labels and Distance Measurements in Biomolecules. In *Electron Paramagnetic Resonance*; Gilbert, B. C., Chechik, V., Murphy, D. M., Eds. 2015; Vol. 24, p 1-31.

(34) Liu, W. M., Overhand, M., Ubbink, M. The Application of Paramagnetic Lanthanoid Ions in Nmr Spectroscopy on Proteins. . *Coord. Chem. Rev.* **2014**, *273*, 2-12.

(35) Koehler, J.; Meiler, J. Expanding the Utility of Nmr Restraints with Paramagnetic Compounds: Background and Practical Aspects. *Prog. Nucl. Magn. Reson. Spectrosc.* **2011**, *59*, 360-389.

(36) Keizers, P. H.; Ubbink, M. Paramagnetic Tagging for Protein Structure and Dynamics Analysis. *Prog. Nucl. Magn. Reson. Spectrosc.* **2011**, *58*, 88-96.

(37) Su, X. C.; Otting, G. Paramagnetic Labelling of Proteins and Oligonucleotides for Nmr. *J. Biomol. NMR* **2010**, *46*, 101-112.

(38) Otting, G. Protein Nmr Using Paramagnetic Ions. *Annu Rev Biophys* **2010**, *39*, 387-405.

(39) Otting, G. Prospects for Lanthanides in Structural Biology by Nmr. *J. Biomol. NMR* **2008**, *42*, 1-9.

(40) Graham, B.; Loh, C. T.; Swarbrick, J. D.; Ung, P.; Shin, J.; Yagi, H.; Jia, X.; Chhabra, S.; Barlow, N.; Pintacuda, G.; Huber, T.; Otting, G. Dota-Amide Lanthanide Tag for Reliable Generation of Pseudocontact Shifts in Protein Nmr Spectra. *Bioconjug Chem* **2011**, *22*, 2118-2125.

(41) Loh, C. T.; Ozawa, K.; Tuck, K. L.; Barlow, N.; Huber, T.; Otting, G.; Graham, B. Lanthanide Tags for Site-Specific Ligation to an Unnatural Amino Acid and Generation of Pseudocontact Shifts in Proteins. *Bioconjug Chem* **2013**, *24*, 260-268.

(42) Dunbrack, R. L., Jr.; Cohen, F. E. Bayesian Statistical Analysis of Protein Side-Chain Rotamer Preferences. *Protein Sci.* **1997**, *6*, 1661-1681.

(43) Barak, N. N.; Neumann, P.; Sevvana, M.; Schutkowski, M.; Naumann, K.; Malesevic, M.; Reichardt, H.; Fischer, G.; Stubbs, M. T.; Ferrari, D. M. Crystal Structure and Functional Analysis of the Protein Disulfide Isomerase-Related Protein Erp29. *J. Mol. Biol.* **2009**, *385*, 1630-1642.

(44) Liepinsh, E.; Baryshev, M.; Sharipo, A.; Ingelman-Sundberg, M.; Otting, G.; Mkrtchian, S. Thioredoxin Fold as Homodimerization Module in the Putative Chaperone Erp29: Nmr Structures of the Domains and Experimental Model of the 51 Kda Dimer. *Structure* **2001**, *9*, 457-471.

(45) M. D. Lee, C.-T. L., J. Shin, S. Chhabra, M. L. Dennis, G. Otting, J. D. Swarbrick, B. Graham, *Chem. Sci.* **2015**, *6*, 2614–2624.

(46) Jeschke, G.; Chechik, V.; Ionita, P.; Godt, A.; Zimmermann, H.; Banham, J.; Timmel, C. R.; Hilger, D.; Jung, H. Deeranalysis2006 - a Comprehensive Software Package for Analyzing Pulsed Eldor Data. *Appl. Magn. Reson.* **2006**, *30*, 473-498.

(47) Mchaourab, Hassane S.; Steed, P. R.; Kazmier, K. Toward the Fourth Dimension of Membrane Protein Structure: Insight into Dynamics from Spin-Labeling Epr Spectroscopy. *Structure* **2011**, *19*, 1549-1561.

(48) Prisner, T. F.; Marko, A.; Sigurdsson, S. T. Conformational Dynamics of Nucleic Acid Molecules Studied by Peldor Spectroscopy with Rigid Spin Labels. *J. Magn. Reson.* **2015**, *252*, 187-198.

(49) Polyhach, Y.; Bordignon, E.; Jeschke, G. Rotamer Libraries of Spin Labelled Cysteines for Protein Studies. *Phys. Chem. Chem. Phys.* **2011**, *13*, 2356-2366.

(50) Kazmier, K.; Sharma, S.; Quick, M.; Islam, S. M.; Roux, B.; Weinstein, H.; Javitch, J. A.; Mchaourab, H. S. Conformational Dynamics of Ligand-Dependent Alternating Access in Leut. *Nat Struct Mol Biol* **2014**, *21*, 472-479.

(51) Kazmier, K.; Sharma, S.; Islam, S. M.; Roux, B.; Mchaourab, H. S. Conformational Cycle and Ion-Coupling Mechanism of the Na+/Hydantoin Transporter Mhp1. *Proc Natl Acad Sci U S A* **2014**, *111*, 14752-14757.

(52) Lelli, M.; Pintacuda, G.; Cuzzola, A.; Di Bari, L. Monitoring Proton Dissociation and Solution Conformation of Chiral Ytterbium Complexes with near-Ir Cd. *Chirality* **2005**, *17*, 201-211.